Lawrence Berkeley National Laboratory

Title
Induced water condensation and bridge formation by electric fields in Atomic Force Microscopy

Permalink
https://escholarship.org/uc/item/6zg528p7

Authors
Sacha, G.M.
Verdaguer, A.
Salmeron, M.

Publication Date
2006-02-22

Peer reviewed

Induced water condensation and bridge formation by electric fields in Atomic Force Microscopy

G. M. Sacha, A. Verdaguer and M Salmeron.

Materials Science Division. Lawrence Berkeley National Laboratory, University of California, Berkeley, California 94720
e-mail: sgomezmonivas@lbl.gov

ABSTRACT:

We present an analytical model that explains how in humid environments the electric field near a sharp tip enhances the formation of water meniscii and bridges between tip and sample. The predictions of the model are compared with experimental measurements of the critical distance where the field strength causes bridge formation

INTRODUCTION

The formation of nanometer-sized water bridges between an Atomic Force Microscope (AFM) tip and a sample is a phenomenon that has produced a great interest in the last years. New applications in imaging and nanofabrication have driven efforts to understand nanometer-size capillarity.[1,2,3] Capillary transport of molecules from the AFM tip to the solid substrate has been used by Piner et al.[4] to "write" patterns of molecules of submicrometer dimensions[5]. Water bridges play also an important role in contacts between objects, where it affects friction and energy dissipation[6].

The interest in the topic has spurned theoretical efforts to model different aspects of capillarity meniscus formation between a tip and a surface[7], structured pores[8], capillary forces between spherical particles and substrates[9], between surfaces[10] and also the kinetics of capillary condensation[11]. Most models are based on macroscopic approximations[12][13] (MIA), molecular level grand canonical Monte Carlo Simulations[14] and Density Functional Theory[15], all of them involving substantial computational effort.

In this paper we develop a simple analytical expression that can be used to determine in a quantitative way the presence and shape of the water film that forms between tip and sample in humid environments. This film grows under the influence of the electric field forming a meniscus that becomes unstable when a critical field is reached, at which point it suddenly forms a bridge between tip and surface. In AFM the capillary force bends the lever, which for small spring

constants can bring the tip in contact with the surface. This is observed experimentally as a sudden jump-to-contact. Our approximation allows us to determine the distance and the voltage at which this capillary jump takes place. Apart from providing a simple way to calculate the critical field and distance it improves our understanding of the mechanisms of water induced jump-to-contact, which is important in non-contact AFM imaging in humid environments.[16]

After presenting the model we will compare its predictions to experimental values of the jump-to-contact distances as a function of humidity and electric field.

THEORETICAL MODEL

In the model the system is assumed to be an axially symmetric metallic tip in the shape of a truncated cone or pyramid of length L and semi-angle θ, terminated with a spherical cap of radius R. Its axis is perpendicular to a flat metallic sample (figure 1). Tip and sample surfaces are assumed to be covered with an initial water layer in equilibrium with the ambient humidity *H*. In the absence of electric fields this film conforms to the surface geometry. The thickness of this initial layer is not important. The profile of this film on the sample surface is represented by the function z(r), where z is the distance to the metallic surface and r is the lateral distance to the tip apex. Although a similar film can also exist on the tip, it will be neglected for simplicity.

Due to its high dielectric constant the water film is assumed to act as a conductor so that its potential is the same as that of the metallic sample. Under these conditions, the condensation energy U_c of the water film is given by:

$$U_c = 2\pi KT \frac{\rho}{m} \ln\left(\frac{1}{H}\right) \int_0^\infty z(r) r dr \quad (1)$$

where ρ and m are the density and mass of water, respectively. In the absence of electric field $z(r)$ should be a plane, but under an applied potential this simple geometry deforms into a different shape.

In the presence of a field E the electrostatic energy of the system U_e can be expressed as[17]:

$$U_e = -\frac{\varepsilon_0}{2} \int_V \frac{\varepsilon-1}{\varepsilon} E_0^2 dV \quad (2)$$

where V is the volume of condensed water, ε the dielectric constant of the liquid and E_0 the electric field before water film condensation. It has been shown[18] that for metallic samples the electrostatic field can be approximated by that produced by a sphere of radius R at a voltage V, which is given by a set of point charges inside the tip:

$$E_0 = -2RV \sum_{i=1}^\infty \frac{\tilde{q}_i}{\tilde{r}_i^2} \quad (3)$$

with the values of q_i and r_i given by the image charge series of a sphere in front of a plate[19]. Combining these equations we obtain the electrostatic energy for a generic function $z(r)$:

$$U_e = -4\pi\varepsilon_0 R^2 V^2 \int_0^\infty \frac{\varepsilon-1}{\varepsilon} z(r) r \left(\sum_{i=1}^\infty \frac{\tilde{q}_i}{\tilde{r}_i^2} \right)^2 dr \quad (4)$$

When water condenses to form a film, U_e decreases and U_c increases. The film profile is determined by minimization of the total energy $U_{tot} = U_e + U_c$. Since along the vertical axis through the tip the field E is minimum at the liquid surface, the electrostatic energy should decrease when the film thickness h increases. Since this field is also a maximum relative to the rest of the surface, water will start condensing at this location. When the electric field reaches a threshold value at a voltage V_{th}, condensation will accelerate because E increases when h increases, until the liquid surface contacts the tip. In this simple approximation the field $E_0 = E(z=0, r=0)$ is the key parameter to obtain V_{th}. Assuming that E_0 is constant over the whole liquid volume, the electrostatic energy is:

$$U_e = -4\pi\varepsilon_0 R^2 V^2 \frac{\varepsilon-1}{\varepsilon} \left(\sum_{i=1}^\infty \frac{\tilde{q}_i}{\tilde{z}_i^2} \right)^2 \int_0^\infty z(r) r \, dr \quad (5)$$

The total energy $U_{tot} = U_e + U_c$ must be negative to induce the formation of a liquid bridge, i.e. the electrostatic energy gain must be larger than the condensation energy. V_{th} can be then obtained from $U_{tot} = 0$:

$$V_{th}^2 = \frac{KT\rho_m}{2R^2 m_m} \frac{\varepsilon}{\varepsilon-1} \left(\sum_{i=1}^\infty \frac{\tilde{q}_i}{\tilde{z}_i^2} \right)^{-2} \ln(1/H) \quad (6)$$

From V_{th} the threshold electric field to induce formation of liquid bridges can be calculated:

$$E_{th} = \sqrt{\frac{2KT\rho_m \varepsilon \ln(1/H)}{m_m \varepsilon_0 (\varepsilon - 1)}} \qquad (7)$$

For large tip radii, $E_{th} = V_{th} / D_b$, where D_b is the distance at which the water bridge forms, causing a jump-to-contact event. For small radii, the threshold voltage and bridge distance do no scale linearly and equation 6 should be used.

For water this equation takes the form $E_{th} = 3.5 \ (\ln(1/H))^{1/2}$ Volts/nm. Threshold voltages for the formation of water necks calculated using equation 6 are shown in Figure 2 as a function of tip-sample separation (a) and humidity (b), and compared with published data from Garcia et al.[20] As can be seen the agreement with the experimental data is very good. Although the assumption of a flat film is sufficient to predict a reasonable value for V_{th}, it cannot explain the effects that result from the real shape of the water meniscus before the bridge is formed. The fact that U_e and U_c have the same dependence with $z(r)$ (both are proportional to the volume), implies that the water surface profile cannot be obtained from the above formula alone. To obtain $z(r)$ two additional contributions to the energy need to be included. One is the van der Waals energy U_{VdW}, and the other the surface tension of water, U_s. Since the van der Waals force is short-range, its contribution will be important only when the distance between the water film and the metallic sample is a few angstroms. Assuming that the two surfaces are almost planar, U_{VdW} can be written as:

$$U_{VdW} = \int_0^\infty \frac{|A|r}{6\pi(r)^2} dr \qquad (8)$$

where A is the Hamaker constant. The capillarity term U_s appears due to the increase of the water surface area when the initially flat layer produces a bulging meniscus under the tip. The surface tension contribution is:

$$U_s = \int_0^\infty 2\pi \alpha r \sqrt{1+z'^2}\, dr \qquad (9)$$

where $\alpha = 73$ mN/m is the surface tension of water and z' the slope of $z(r)$. Using these contributions together with the electrostatic energy U_e, the profile $z(r)$ is obtained by minimization of the total energy:

$$\frac{\partial U_{tot}}{\partial z(r)} - \frac{d}{dr}\frac{\partial U_{tot}}{\partial z'(r)} = 0 \qquad (10)$$

where $U_{tot} = U_e + U_{VdW} + U_C + U_s$.

The functional dependence of the electrostatic field is not easy to calculate because it depends on the entire function $z(r)$. For that reason we use the Radial Field Approximation (RFA), which assume that the electric field is the same as that inside a spherical capacitor, with the spherical tip being the central electrode[20].

In figure 3a we show water profiles obtained using the RFA. The profile barely changes until the voltage is close to V_{th}. In the case shown in the figure it changes appreciably only when the voltage is larger than 7V, which produces a bulge of a few angstroms, i.e., one or two water layers.

As the voltage gets closer to the threshold any small perturbation can precipitate the formation of a bridge. Figure 3b shows the height of the film under the tip as a function of voltage for different relative humidities. The height diverges when $V = V_{th}$. The initial water thickness was obtained in this case from the balance between van der Waals and condensation energies[21].

EXPERIMENTAL SECTION

In AFM experiments the threshold distance for bridge formation can be determined from the jump-to-contact as the tip approaches the surface with different applied voltages. This jump however must be distinguished from that due to pure mechanical instability of the cantilever spring. This occurs at the point where the slope of the force-distance curve is equal to the cantilever spring constant K. Assuming that the electrostatic force follows a 1/D dependence, as shown in reference[22], the mechanical instability jump-to-contact distance D_{mech} can be easily calculated. The expression in nanometer units is:

$$D_m(nm) = 0.1667\sqrt{\frac{R(nm)}{K(N/m)}}V(V) \qquad (11)$$

Depending on tip radius, spring constant, applied voltage and relative humidity, bridge formation or mechanical instability will be responsible for the jump-to-contact. Since this quantity is readily accessible in AFM studies, we used it to test the above theories.

The experiments were carried out at room temperature ($22 \pm 2^{o}C$) with a home-built AFM[23] controlled by RHK electronics. The microscope was enclosed in a glove box where humidity

control was achieved by circulating dry N_2 to decrease the humidity (H) or by bubbling the N_2 through de-ionized water to increase the humidity. Humidity and temperature were measured using a Thermo-hygrometer from RadioShack. Values from 10% to 80% could be maintained with a variation of ±1% per hour. The absolute values of H have an uncertainly of ±5%. Tips from Ultrasharp Mikromash coated with conductive TiN were used with cantilever spring constants of 9 N/m, as determined using Sader's method[24].

Figure 4 shows the measured jump-to-contact distances (normalized to the bias voltage) over a gold surface and their dependence on humidity for various applied voltages. We also show the calculated curves of D_b (due to water bridge formation) and D_m (due to mechanical instability). As mention above, the threshold voltage and the distance D_b of bridge formation do not scale proportionally, so that the calculated curves (dashed lines) do not coincide exactly. At 6 V the two lines cross at around 40%RH. Below that value, D_m is smaller than D_b, indicating that the humidity is too low to produce a water meniscus before the tip jumps to the surface due to the mechanical instability. Above 40% RH meniscus and bridge formation occur before the mechanical instability.

In figure 5a we show the measured Force vs D curve for a low relative humidity (20%), where the jump to contact is due to the mechanical instability, which occurs at 4.4 nm. The inset shows the force as a function of 1/D, which gives a strait line with a slope directly related to the tip radius. In the present case R=126±10nm.

In figure 5b we show another F vs D curve with the same tip but at higher humidity (67%). In this case the tip jumps to the surface because of the formation of a water bridge, as shown by the value of F' which is smaller than the spring constant of the cantilever.

CONCLUSION

We have developed a simple analytical approximation that makes it possible to analyze quantitatively the effect of the enhanced water condensation due to the electric field. The theory gives the threshold voltage for bridge formation with excellent accuracy.

ACKNOWLEDGEMENT

Figure captions:

Fig 1. Tip-sample geometry with a water film (blue) used in the theoretical treatment. Humidity (H) induces water condensation on the substrate with a surface profile characterized by the function z(r).

Figure 2: Threshold voltage for the formation of a water bridge as a function of tip-sample distance (a), and as a function of relative humidity (b). Dots are experimental results from ref. 19

Figure 3: a) Water meniscus profile calculated for different voltages by minimization of the energy. Tip radius R=50 nm; distance D=7 nm; humidity H=30%. The last stable solution is found at V=9V. An increment of the voltage over this value produces a water bridge. b) Height of the meniscus under the tip apex ($\rho=0$ in figure 4a) for different values of the relative humidity. R_{tip}=50nm, d=7nm.

Figure 4: Jump-to-contact distance normalized to the bias voltage for a TiN tip approaching a gold surface at different voltages as a function of relative humidity. Lines are drawn for the theoretically predicted bridge threshold formation values D_b (dashed lines) and for the mechanical instability D_m (solid horizontal lines). The two horizontal lines correspond to the average distance D and the distance of closest approach due to the noise (D- ΔD). Tip R=126nm.

Figure 5: a) Electrostatic force vs tip-sample distance for a relative humidity of 20% and a bias voltage of 6V. The inset shows the force vs 1/D, a strait line with a slope proportional to the tip radius, 126nm in this case. The mechanical instability (jump-to-contact) occurs at 4.4 nm, where the

slope is indeed very close to the cantilever spring constant. b) Electrostatic force vs tip-sample distance for a relative humidity of 67% and V=4V. The jump-to-contact occurs at 4nm. At this distance, the force derivative F' is smaller than the cantilever spring constant, indicating that the jump-to-contact is due to the formation of a water bridge
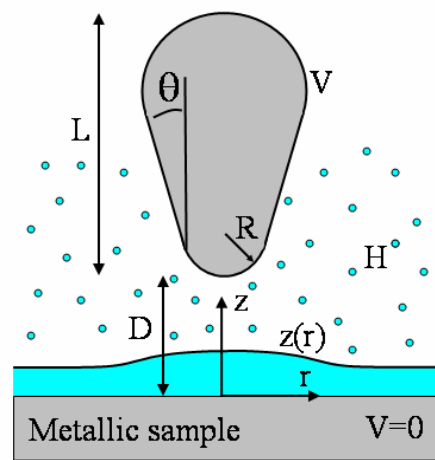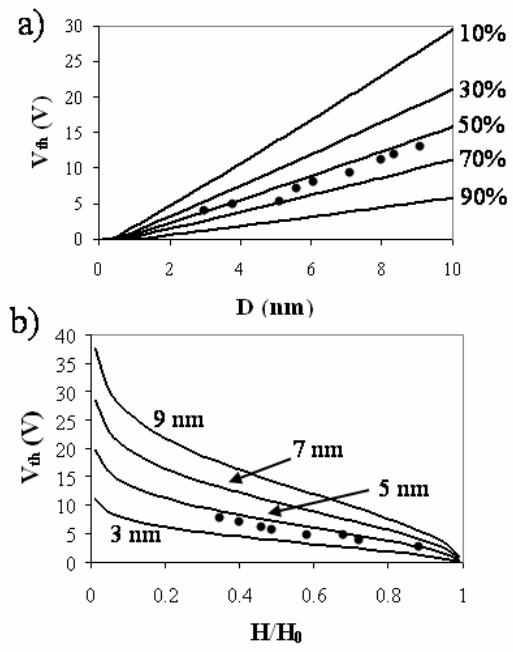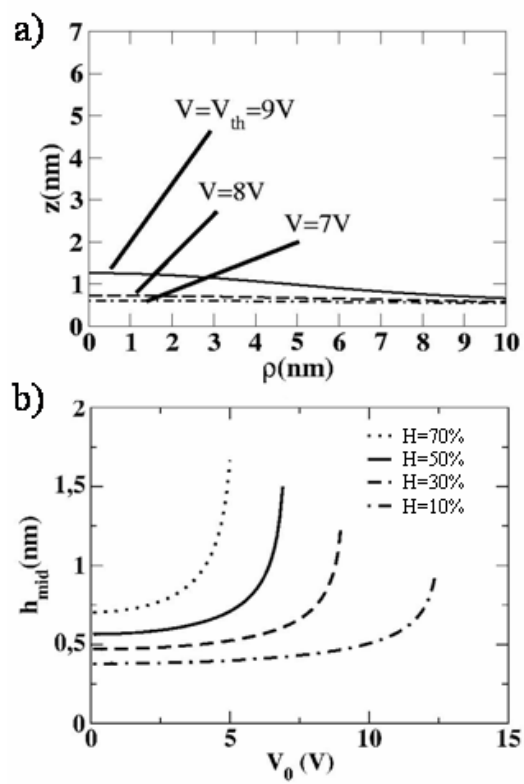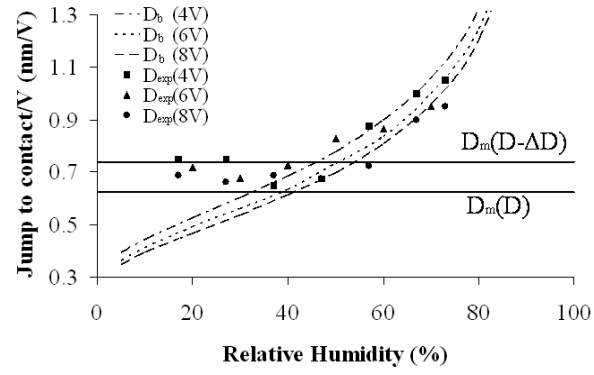
Figure 1

Figure 2

Figure 3

Figure 4

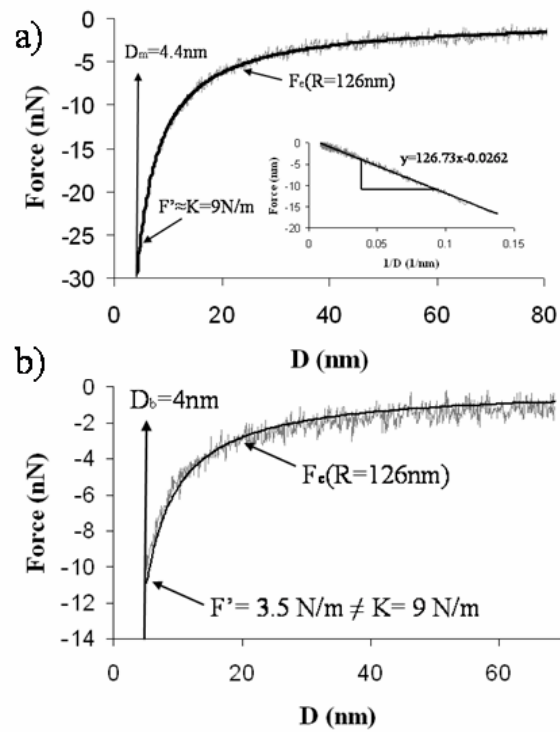Figure 5

[1] Thundat, T.; Zheng, X.Y.; Chen, G.Y. and Warmack, R.J. *Surf. Sci.* **1993,** 294, L939.

[2] Morimoto,K.; Araki, K.; Yamashita, K.; Morita, K. and Niwa, M. *Appl. Surf. Sci.* **1997,** *117-118,* 652.

[3] Dagata J. A.; Pérez-Murano F.; Martín C.; Kuramochi H. and Yokohama H. *J. Appl. Phys.* **2004,** 96, 2393.

[4] Piner, R.D.; Zhu, J.; Xu, F.; Hong, S. and Mirkin, C.A. *Science* **1999,** *283,* 661.

[5] Lee, K.-B.; Park, S.-J.; Mirkin, C.A.; Smith, J.C. and Mrksich, M. *Science,* **2002,** *295,* 1702 .

[6] Szoszkiewicz R. and Riedo E. *Phys. Rev. Lett.* **2005,** 95, 135502. Szoszkiewicz R. and Riedo E. *Appl. Phys. Lett.* **2005,** 87, 033105

[7] Gao, C. *Appl. Phys. Lett.* **1997,** *71,* 1801.

[8] Valencia, A.;Brinkmann, M. and Lipowsky, R. *Langmuir* **2001,** *17*, 3390.

[9] de Lazzer, A.; Dreyer, M. and Rath., H.J. *Langmuir* **1999,** *15,* 4551.

[10] Restagno, F.; Bocquet, L. and Bilben, T. *Phys. Rev. Lett.* **2000,** *84*, 2433.

[11] Kohonen, M.; Maeda, N. and Christenson, H. K. *Phys. Rev. Lett.* **1999,** *82*, 4667.

[12] Stifter T.; Marti O. and Bhushan B. *Phys. Rev. B.* **2000**, 62, 13667

[13] Gómez-Moñivas, S.; Sáenz, J.J.; Calleja, M. and García, R. *Phys. Rev. Lett.* **2003,** *91*, 56101.

[14] Jang J.; Schatz G. and Ratner M. *Phys. Rev. Lett.* **2004,** 92, 085504.

[15] Paramonov P. V. and Lyuksyutov S. F. *J. Chem. Phys.* **2005,** 123, 084705.

[16] Capella B. and Dietler G. *Surf. Science Rep.* **1999** 34, 1. Piner R. and Mirkin C. *Langmuir* **1997,** 13, 6864.

[17] Gómez-Moñivas, S.; Sáenz, J.J.; Carminati, R. and Greffet, J.J. *Appl. Phys. Lett.* **2000,** *76,* 2955.

[18] Gómez-Moñivas, S.; Froufe-Pérez, L.S.; A.J. Camaño, A.J.; J.J. Saenz, J.J. *Appl. Phys. Lett.* **2001**,*79,* 4048.

[19] J. D. Jackson. *Classical electrodynamics.* J. Wiley (1975)*.*

[20] García, R.; Calleja, M. and Rohrer, H. *J. Appl. Phys.* **1999,** *86,* 1898.

[21] Israelachvili, J.N. *Intermolecular and Surface Forces 2nd ed* **1991**, (New York: Academic).

[22] Sacha, G.M.; Verdaguer, A.; Martínez, J.; Ogletree, D.F. and Salmeron, M. *Appl. Phys. Lett.* **2005,** *86,* 123101.

[23] H. Bluhm, S.H. Pan, L. Xu, T.Inoue, D.F. Ogletree, M. Salmeron, *Rev Sci Intrum.* **1998**, *69,* 1781.

[24] J. E. Sader, J. W. M. Chon and P. Mulvaney, Rev. Sci. Instrum., **1999,** 70, 3967.